

SUPPORTING INFORMATION

Tuning the Selectivity of Single-Site Supported Metal Catalysts with Ionic Liquids

Melike Babucci,^{†,‡} Chia-Yu Fang,[‡] Adam S. Hoffman,^{‡,§} Simon R. Bare,[§] Bruce C. Gates,[‡]
and Alper Uzun^{*,†,‡}

[†]Department of Chemical and Biological Engineering, Koç University, Rumelifeneri Yolu, Sariyer 34450, Istanbul, Turkey

[‡]Koç University TÜPRAŞ Energy Center (KUTEM), Koç University, Rumelifeneri Yolu, Sariyer 34450, Istanbul, Turkey

[‡]Department of Chemical Engineering, University of California, Davis, CA 95616, United States

[§]SSRL, SLAC National Accelerator Laboratory, Menlo Park, CA, 94025 United States

*Corresponding Author: auzun@ku.edu.tr

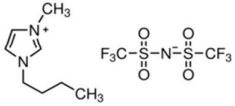
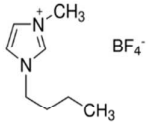
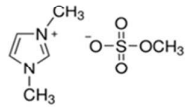
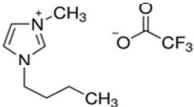
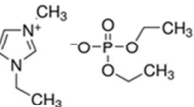
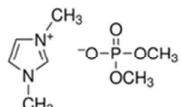
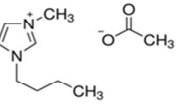
Experimental

Materials and Methods

All chemicals (precursors, aluminum oxide, and ILs) were purchased from Sigma-Aldrich with the highest available purities. All ILs were dried at 353 K for 6 h and kept under vacuum for 12 h before transfer to an argon-filled Labconco glove box. Site-isolated supported iridium complexes were prepared by the reaction of $\text{Ir}(\text{CO})_2(\text{acac})$ (acac = acetylacetonate) precursor (35.8 mg) with $\gamma\text{-Al}_2\text{O}_3$ (992 mg) which was calcined in flowing O_2 with a temperature ramp rate of 3 K/min from room temperature to 773 K and held for 5 h, using air exclusion techniques.¹ The precursor and support (with an iridium loading of 1 wt.%) were slurried in *n*-pentane, which had been purified by an SBS-MBraun solvent purifier. The slurry was mixed for one day followed by evacuation for solvent removal. The resultant solid catalyst was stored in the glove box. IL-coated supported metal complex catalysts were prepared by immersing the supported metal complex (50 mg) in the IL (40 mg) and by adding an excess amount of calcined support (110 mg) to adsorb remaining unadsorbed IL, with the manipulations done in the glove box. Each resultant sample had approximately 20 and 0.4 wt% IL and iridium loadings, respectively. All the IL-coated and uncoated samples were stored in the glove box under argon.

A list of 1,3-dialkylimidazolium ILs used in this work is provided in Table S1.

Table S1. Names, abbreviations, and structures of the ILs.

IL Name	Abbreviation	IL Structure
1-Butyl-3-methylimidazolium bis(trifluoromethylsulfonyl)imide	[BMIM][NTf ₂]	
1-Butyl-3-methylimidazolium tetrafluoroborate	[BMIM][BF ₄]	
1,3-Dimethylimidazolium methyl sulfate	[DMIM][MSO ₄]	
1-Butyl-3-methylimidazolium trifluoroacetate	[BMIM][TFA]	
1-Ethyl-3-methylimidazolium diethyl phosphate	[EMIM][DEP]	
1,3-Dimethylimidazolium dimethyl phosphate	[DMIM][DMP]	
1-Butyl-3-methylimidazolium acetate	[BMIM][Ac]	

Sample Characterization with Fourier Transform Infrared (FTIR) Spectroscopy

A Bruker Vertex 80v spectrometer with a vacuum sample chamber was used in transmission mode to measure IR spectra with a spectral resolution of 2 cm^{-1} . Each sample was pressed between two KBr windows in the glove box. IR spectra of samples were recorded with exclusion of moisture and air at room temperature. For each measurement, 256 scans were averaged, and before each of these a background of 128 scans was collected. Stretching vibrations of carbonyl groups, $\nu(\text{CO})$, of the metal oxide-supported $\text{Ir}(\text{CO})_2$ complexes were used to probe the electronic environment of the iridium centers.

High-Energy Resolution Fluorescence Detection X-Ray Absorption Near Edge Structure (HERFD XANES) Measurements

HERFD XANES measurements were collected at Beamline 6-2 at the Stanford Synchrotron Radiation Lightsource (SSRL). A liquid-nitrogen-cooled double-crystal Si(311) monochromator was equipped to select the energy of the incident beam with a flux of 3×10^{12} photons \times s^{-1} . A Rowland circle spectrometer (radius 1 m) equipped with three spherically bent Si(800) analyzers and a silicon drift detector were used to select the Ir L α (9175 eV) emission line with a measured resolution of 1.3 eV. An iridium foil was scanned in the transmission mode for energy calibration. Each sample (less than 100 mg in mass) was loaded into a static cell, which was sealed in an argon-filled glovebox, preventing contamination by water and oxygen. The iridium loading of each sample was less than 0.5 wt. % to minimize self-absorption, and all HERFD-XANES spectra were measured within 2 min with each sample being scanned three to six times to improve signal-to-noise ratio. A reference material was not scanned simultaneously with the samples.

The analysis of the HERFD XANES data was carried out with the software ATHENA of the IFEFFIT package.^{2,3} The edge, determined by first inflection point of the absorption edge of the Ir foil, was calibrated to the reported Ir L III energy, 11215 eV. This calibration was used to calibrate a known glitch in the monochromator observed in the I_0 signal of each scan. A least-squares Gaussian fit of the glitch, determined the error in the energy calibration of the samples to be 22 meV/0.022 eV. Energy calibration was achieved by aligning the glitch in each scan to the glitch in the Ir foil reference scans. Three to six scans per sample were averaged with the averaged spectra being used for deglitching and normalization. The averaged spectrum was processed by fitting a second-order polynomial to the pre-edge region and subtracting this from the entire spectrum. Edge energy was determined by the first derivative of the normalized absorbance. The data were normalized by dividing the absorption intensity by the height of the absorption edge.

Catalyst performance measurements

For catalyst performance measurements, uncoated and IL-coated supported iridium complexes (each including 150-250 mg of iridium dicarbonyl complexes) were placed into a $\frac{1}{4}$ -in. stainless steel once-through tubular flow reactor. A three-zone resistively heated furnace (Thermcraft, model # XST-3-0-18-3V) equipped with PC-operated temperature controllers was utilized for temperature control in the reactor. Electronic mass flow controllers (Aalborg, model GFC17) were used to adjust the flow rates of gases. Before each measurement, samples were treated in flowing ethene (50 vol% in balance helium, Linde) at 373 K with a ramp rate of 3 K/min for 1 h to convert the almost inactive supported $\text{Ir}(\text{CO})_2$ complexes into mixtures of $\text{Ir}(\text{CO})_2(\text{C}_2\text{H}_4)$ and $\text{Ir}(\text{CO})_2(\text{C}_2\text{H}_4)_2$ complexes, as reported previously for HY-zeolite-supported complexes.⁴

Following a cooling period to the reaction temperature (333 K) in flowing He, the feed was switched to a reaction gas mixture with a molar ratio of 1,3-butadiene (Linde, 99.6 vol%): H_2 (Linde, 99.99 vol%) = 1:2 with the reactor operated at atmospheric pressure and 333 K. Conversions of 1,3-butadiene were in the differential range, <2%. Product analysis was performed using an online gas chromatograph (Agilent GC 7890A) equipped with a GS-Alumina column (50 m \times 530 μm) and a flame ionization detector. Reaction rates are reported per Ir atom in terms of turnover frequencies (TOFs), assuming that all the Ir atoms were accessible for reaction.

Conductor-Like Screening Model for Realistic Solvents (COSMO-RS) calculations

COSMOTermX (version 1601) software with the Ionic Liquid Screening module was used to calculate the solubility of the reactants and products in each IL by setting the temperature to 333 K. Data were analyzed according to a previous study.⁵ The capacity term is defined as the inverse of the activity coefficient at infinite dilution⁶ for each component in each IL, considered as mole fraction in solution. The definition of capacity is as follows:

$$C_i^\infty = \frac{1}{\gamma_i^\infty} \sim x$$

Here, C_i^∞ is the solvent capacity at infinite dilution for components "i" being 1,3-butadiene (BD), butane (B), *trans*-2-butene (T2B), *cis*-2-butene (C2B), 1-butene (1B), and hydrogen (H_2) in each IL at 333 K and γ_i^∞ is the activity in each IL and x is the mole fraction of the gas components in solution.

Supporting Data

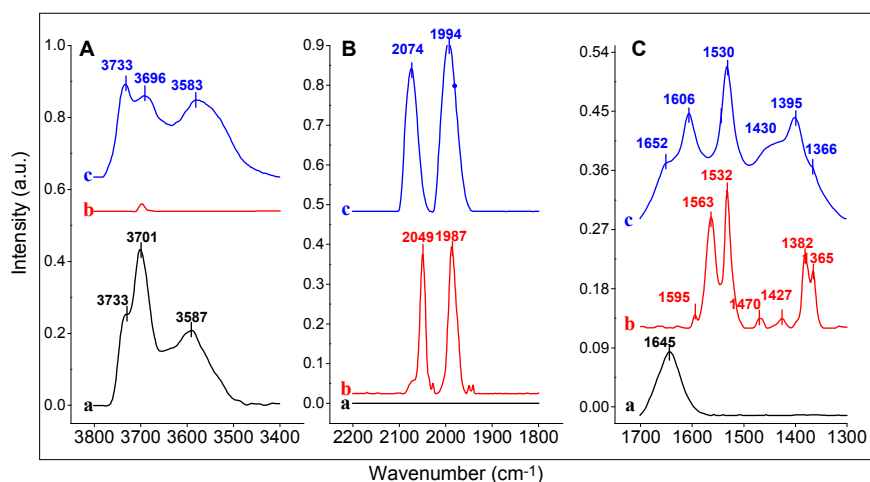


Figure S1. IR spectra of calcined γ - Al_2O_3 (a), precursor $\text{Ir}(\text{CO})_2(\text{acac})$ mixed with KBr (b) and the catalyst formed by reaction of γ - Al_2O_3 with $\text{Ir}(\text{CO})_2(\text{acac})$ (c): in the region of A) 3400–3800 cm^{-1} ; B) 1800–2200 cm^{-1} ; C) 1300–1700 cm^{-1} .

IR spectra given in Figure S1-A indicate that the hydroxyl groups characterized by bands at 3587 and 3693 cm^{-1} belonging to γ - Al_2O_3 were consumed during the sample synthesis. This decrease in intensity of the IR bands suggests the reaction of the precursor with these acidic hydroxyl groups. Moreover, in Figure S1-B, the presence of two distinct $\nu(\text{CO})$ bands, at 1994 and 2074 cm^{-1} , attributed to $\nu(\text{CO})_{\text{asym}}$ and $\nu(\text{CO})_{\text{sym}}$, respectively, in the as-prepared sample confirms the presence of iridium *gem*-dicarbonyl groups. These fingerprints were shifted from those observed in $\text{Ir}(\text{CO})_2(\text{acac})$ mixed with KBr (1987 and 2049 cm^{-1}), indicating that the supported complex is a species different from the precursor. Moreover, in the 1300–1700 cm^{-1} region, mostly showing the IR bands of acetylacetonate, the IR spectrum of the supported iridium complex (Figure S1-C) includes bands at 1365, 1404, 1460, 1533, and 1608 cm^{-1} . These bands are assigned to $\delta_{\text{s}}(\text{CH}_3)$, $\nu_{\text{asym}}(\text{CO})_{\text{ring}}$, $\delta_{\text{as}}(\text{CH})$, $\nu_{\text{as}}(\text{CCC})_{\text{ring}}$, and $\nu_{\text{sym}}(\text{CO})_{\text{ring}}$, respectively, indicating the IR bands of Hacac adsorbed on γ - Al_2O_3 rather than those of the precursor (1365, 1382, and 1531 cm^{-1}).^{1,7} Thus, we conclude that leaving of the acac ligand from the precursor $\text{Ir}(\text{CO})_2(\text{acac})$ results in the chemisorption of the remaining $\text{Ir}(\text{CO})_2$ complex onto the support. Therefore, we infer that site-isolated iridium *gem*-dicarbonyl complexes were formed.

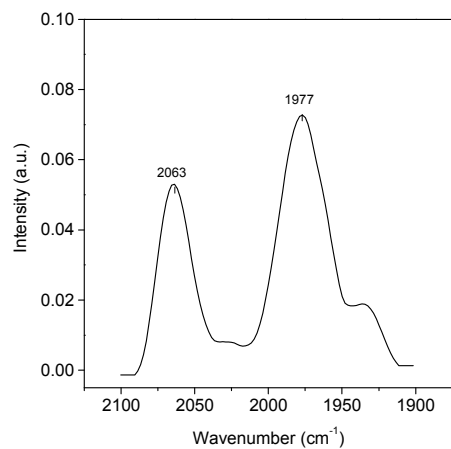


Figure S2. IR spectra characterizing [BMIM][NTf₂]-coated Ir(CO)₂/γ-Al₂O₃ in the region of 1900-2100 cm⁻¹.

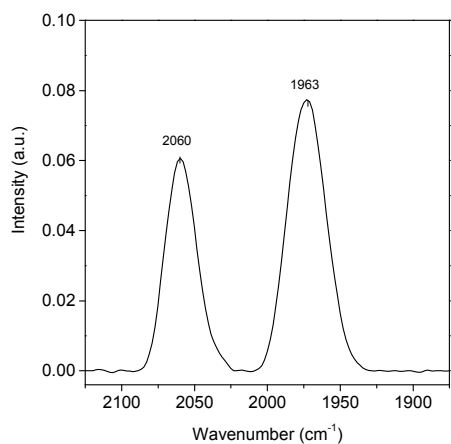


Figure S3. IR spectra characterizing [BMIM][BF₄]-coated Ir(CO)₂/γ-Al₂O₃ in the region of 1900-2100 cm⁻¹.

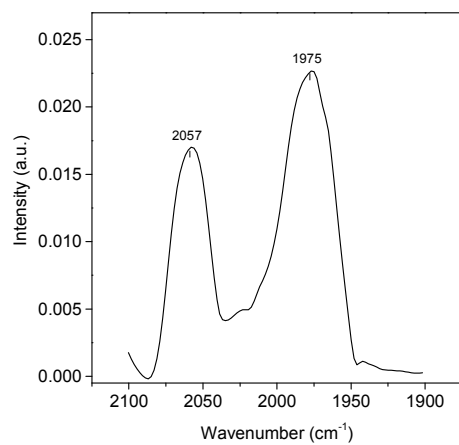


Figure S4. IR spectra characterizing [DMIM][MSO₄]-coated Ir(CO)₂/γ-Al₂O₃ in the region of 1900-2100 cm⁻¹.

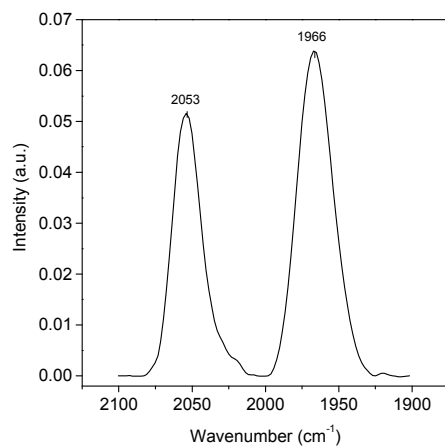


Figure S5. IR spectra characterizing [BMIM][TFA]-coated Ir(CO)₂/γ-Al₂O₃ in the region of 1900-2100 cm⁻¹.

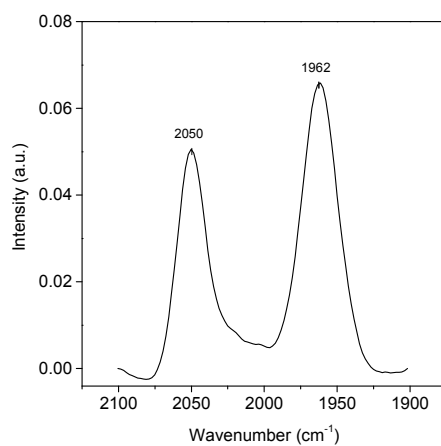


Figure S6. IR spectra characterizing [EMIM][DEP]-coated Ir(CO)₂/γ-Al₂O₃ in the region of 1900-2100 cm⁻¹.

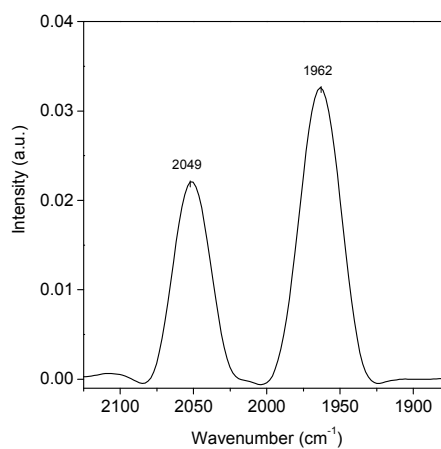


Figure S7. IR spectra characterizing [DMIM][DMP]-coated Ir(CO)₂/γ-Al₂O₃ in the region of 1900-2100 cm⁻¹.

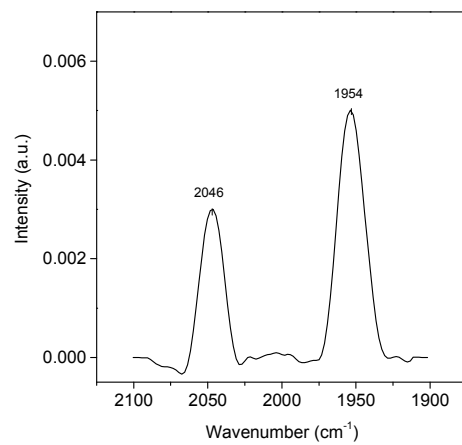


Figure S8. IR spectra characterizing [BMIM][Ac]-coated Ir(CO)₂/γ-Al₂O₃ in the region of 1900-2100 cm⁻¹.

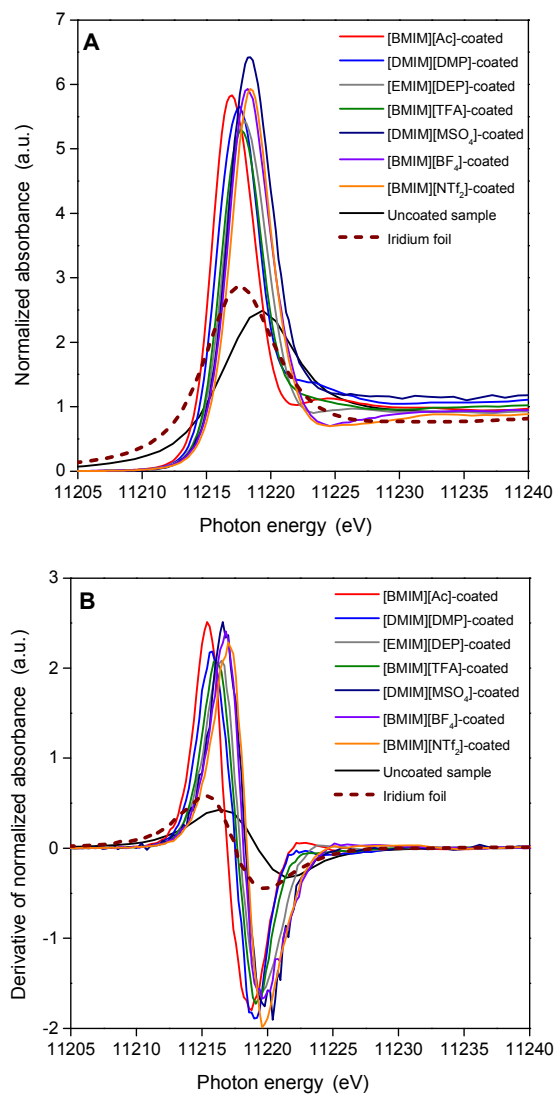


Figure S9. A, Normalized HERFD XANES spectra at the Ir L_{III} edge characterizing Ir(CO)₂/γ-Al₂O₃ complexes coated with various 1,3-dialkylimidazolium ILs (full names of ILs are provided in Table S1, given above). B, Derivatives of the normalized HERFD XANES spectra showing the edge energy positions. For comparison, the spectrum of iridium foil (measured in transmission mode) is provided (dashed brown line).

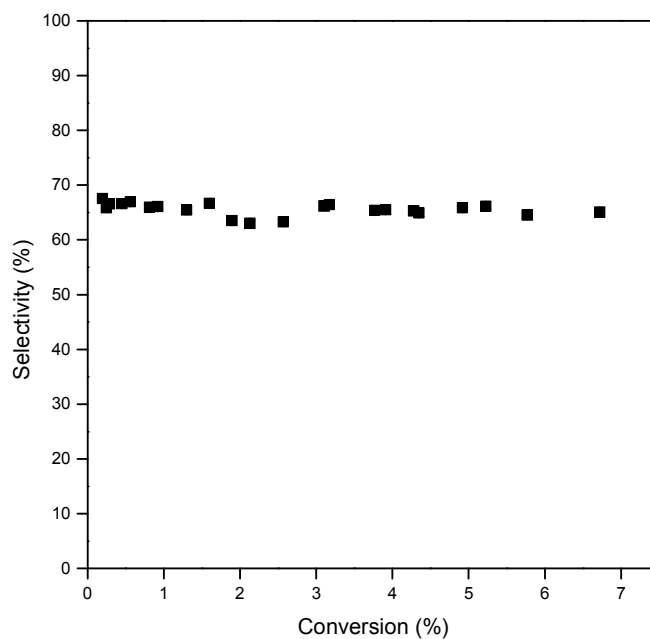


Figure S10. Change in total butene selectivity with BD conversion on a representative catalyst, [EMIM][DEP]-coated $\text{Ir}(\text{CO})_2/\gamma\text{-Al}_2\text{O}_3$.

Table S2. $\nu(\text{C}2\text{H})$ of individual ILs; $\nu(\text{CO})$ bands and edge energy on uncoated and coated $\text{Ir}(\text{CO})_2/\gamma\text{-Al}_2\text{O}_3$ complexes.

IL-coated supported $\text{Ir}(\text{CO})_2$ complexes	$\nu(\text{C}2\text{H})$ (cm^{-1})	$\nu(\text{CO})_{\text{sym}}$ (cm^{-1})	$\nu(\text{CO})_{\text{asym}}$ (cm^{-1})	Edge Energy (eV)
Uncoated sample	-	2074	1994	11217.9
[BMIM][NTf ₂]	3124	2063	1977	11217.0
[BMIM][BF ₄]	3122	2060	1973	11216.8
[DMIM][MSO ₄]	3111	2057	1975	11216.6
[BMIM][TFA]	3090	2053	1966	11216.0
[EMIM][DEP]	3071	2050	1962	11216.1
[DMIM][DMP]	3069	2049	1962	11215.8
[BMIM][Ac]	3056	2046	1954	11215.4

Characterization of Samples Before and After 1,3-Butadiene Hydrogenation

When γ - Al_2O_3 -supported iridium dicarbonyl was exposed to flowing ethene (50 vol% in balance He) at 373 K, changes in IR spectra were observed. In 1900–2100 cm^{-1} region, the intensity of $\nu_{\text{asym}}(\text{CO})$ at 1994 cm^{-1} decreased slightly with appearance of two new bands at 2027 and 2047 cm^{-1} . These new bands are assigned to $\text{Ir}(\text{CO})(\text{C}_2\text{H}_4)$ and $\text{Ir}(\text{CO})(\text{C}_2\text{H}_4)_2$, respectively.^{7,8}

IR spectra given in Figure S9 show changes after BD hydrogenation as well. In the region of 500–1750 cm^{-1} of uncoated species, the peak at 937 cm^{-1} disappeared with the appearance of four new bands, at 1040, 1121, 1223, and 1258 cm^{-1} , assigned to BD and methyl groups physisorbed on iridium. Moreover in the 2800–3800 cm^{-1} region, the band at 3583 cm^{-1} assigned to acidic hydroxyl groups vanished. Instead, the presence of the bands at 2855, 2927, and 2955 cm^{-1} confirm the adsorption of butane $\nu(\text{CH}_2)$, 1-B or T2B/C2B ($\nu_{\text{asym}}(\text{CH}_2)$) and isobutylene or methyl, respectively.⁹

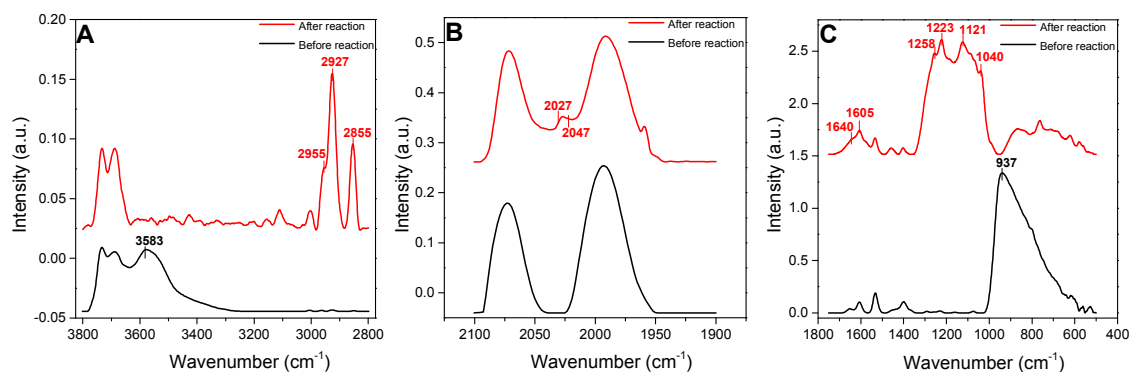


Figure S11. IR spectra of uncoated $\text{Ir}(\text{CO})_2/\gamma\text{-Al}_2\text{O}_3$ before (black) and after (red) 1,3-butadiene hydrogenation in the region of A) 2800–3800 cm^{-1} ; B) 1900–2100 cm^{-1} ; C) 500–1750 cm^{-1} .

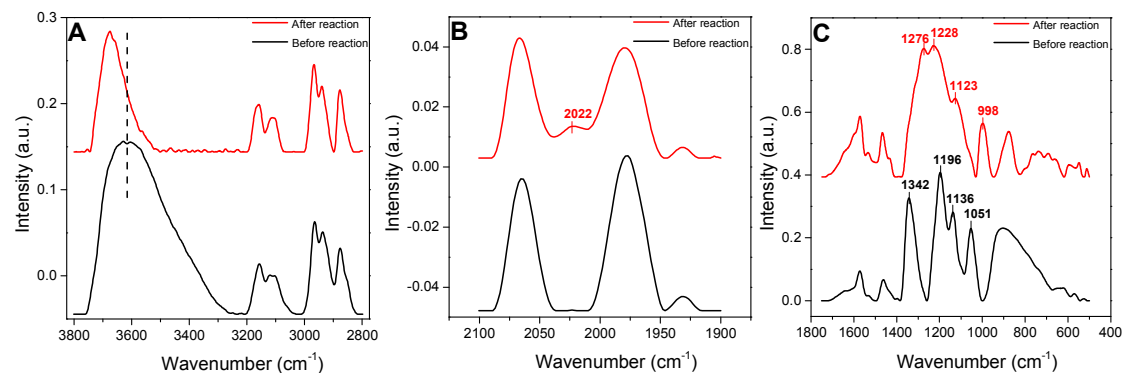


Figure S12. IR spectra of [BMIM][NTf_2]-coated $\text{Ir}(\text{CO})_2/\gamma\text{-Al}_2\text{O}_3$ before (black) and after (red) 1,3-butadiene hydrogenation in the region of A) 2800–3800 cm^{-1} ; B) 1900–2100 cm^{-1} ; C) 500–1750 cm^{-1} .

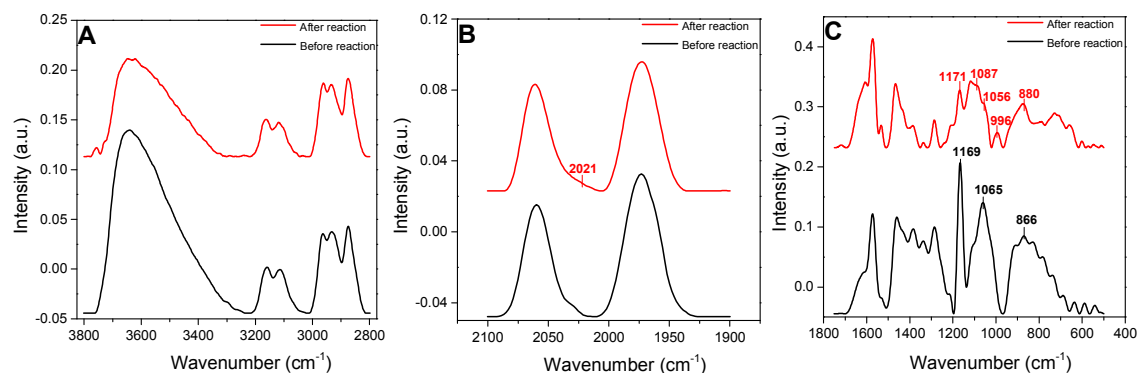


Figure S13. IR spectra of [BMIM][BF₄]-coated Ir(CO)₂/γ-Al₂O₃ before (black) and after (red) 1,3-butadiene hydrogenation in the region of A) 2800–3800 cm⁻¹; B) 1900–2100 cm⁻¹; C) 500–1750 cm⁻¹.

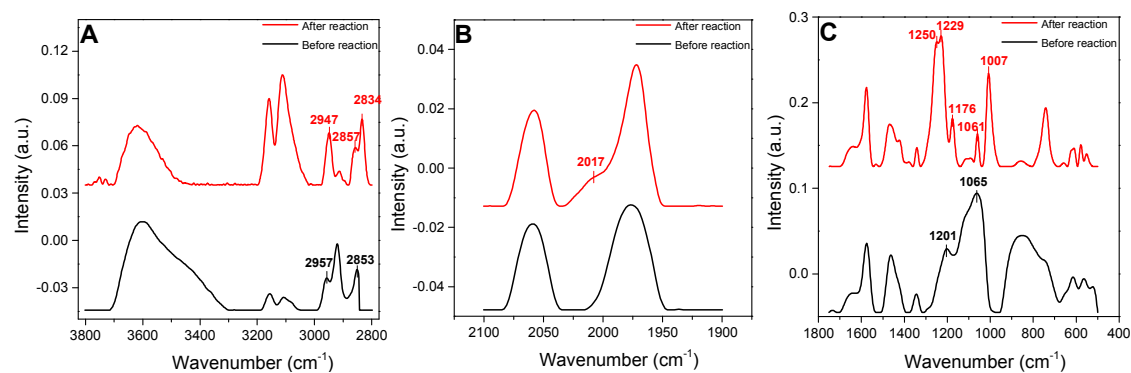


Figure S14. IR spectra of [DMIM][MSO₄]-coated Ir(CO)₂/γ-Al₂O₃ before (black) and after (red) 1,3-butadiene hydrogenation in the region of A) 2800–3800 cm⁻¹; B) 1900–2100 cm⁻¹; C) 500–1750 cm⁻¹.

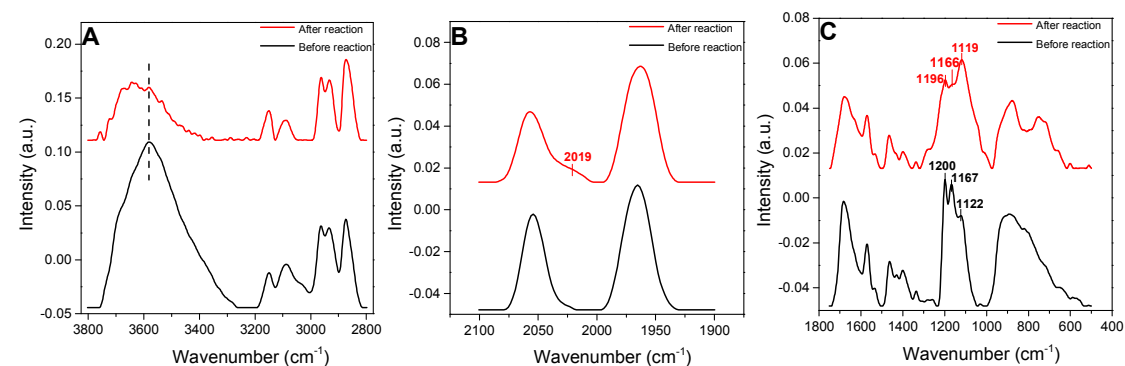


Figure S15. IR spectra of [BMIM][TFA]-coated Ir(CO)₂/γ-Al₂O₃ before (black) and after (red) 1,3-butadiene hydrogenation in the region of A) 2800–3800 cm⁻¹; B) 1900–2100 cm⁻¹; C) 500–1750 cm⁻¹.

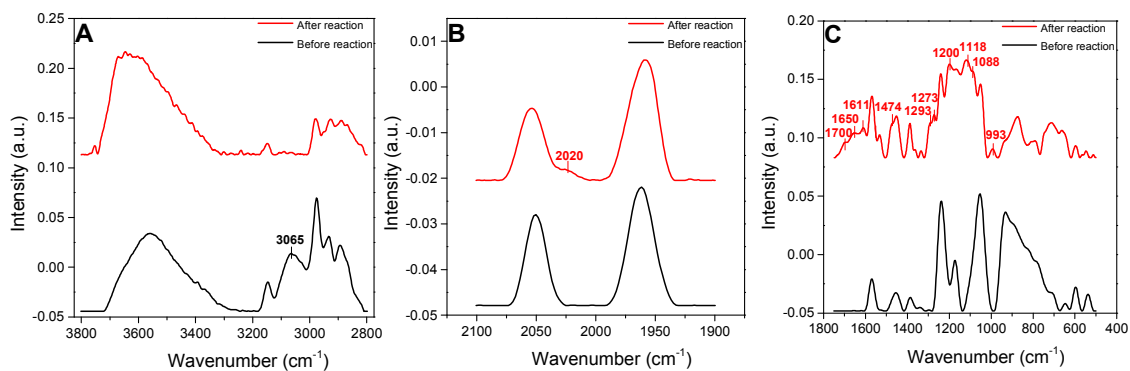


Figure S16. IR spectra of [EMIM][DEP]-coated $\text{Ir}(\text{CO})_2/\gamma\text{-Al}_2\text{O}_3$ before (black) and after (red) 1,3-butadiene hydrogenation in the region of A) 2800–3800 cm^{-1} ; B) 1900–2100 cm^{-1} ; C) 500–1750 cm^{-1} .

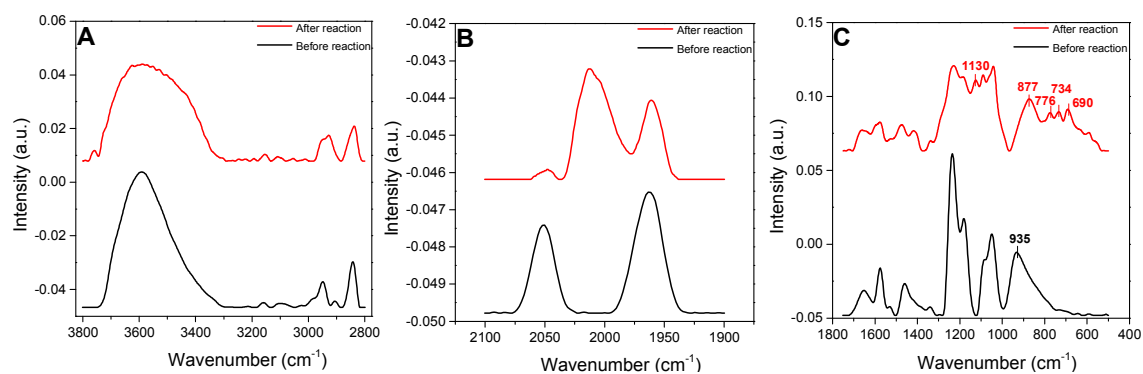


Figure S17. IR spectra of [DMIM][DMP]-coated $\text{Ir}(\text{CO})_2/\gamma\text{-Al}_2\text{O}_3$ before (black) and after (red) 1,3-butadiene hydrogenation in the region of A) 2800–3800 cm^{-1} ; B) 1900–2100 cm^{-1} ; C) 500–1750 cm^{-1} .

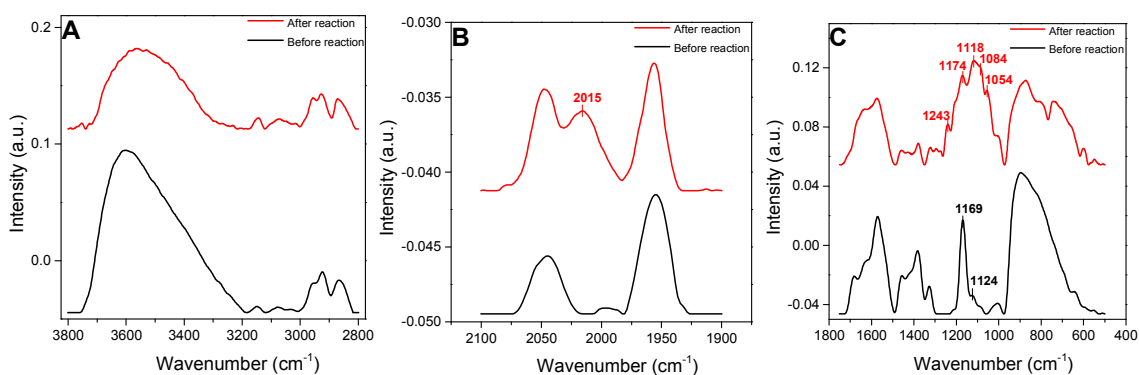


Figure S18. IR spectra of [BMIM][Ac]-coated $\text{Ir}(\text{CO})_2/\gamma\text{-Al}_2\text{O}_3$ before (black) and after (red) 1,3-butadiene hydrogenation in the region of A) 2800–3800 cm^{-1} ; B) 1900–2100 cm^{-1} ; C) 500–1750 cm^{-1} .

Table S3. Selectivities and TOF values for partial hydrogenation of BD at 333 K and 1 bar (BD:H₂ = 1:2, molar) on uncoated and IL-coated ethene-treated Ir(CO)₂ complexes supported on γ -Al₂O₃.

IL-coated supported Ir(CO) ₂ complexes	Selectivity for hydrogenation of 1,3-butadiene at 333 K (%)					TOF (s ⁻¹)	Conversion (%)
	B	T2B	1B	C2B	Total butenes		
Uncoated sample	49	15	24	13	51	0.00838	1.42
[BMIM][NTf ₂]	39	18	32	11	61	0.00436	1.26
[BMIM][BF ₄]	38	17	31	14	62	0.00126	0.82
[DMIM][MSO ₄]	35	20	29	16	65	0.00129	0.95
[BMIM][TFA]	36	20	28	17	64	0.00085	0.91
[EMIM][DEP]	34	20	34	13	66	0.00145	0.78
[DMIM][DMP]	27	19	44	10	73	0.00213	1.02
[BMIM][Ac]	22	22	42	14	78	0.00121	0.86

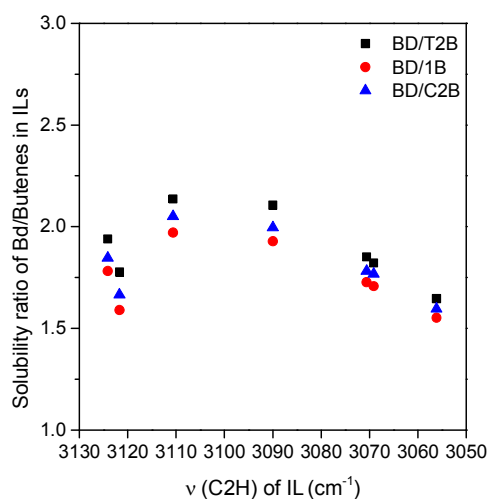


Figure S19. Solubility ratios of BD relative to those of individual butene isomers in ILs as a function of ν (C2H) of corresponding IL.

Table S4. Capacity of individual components (BD, T2B, 1B, C2B, B, and H₂) in ILs at 333 K determined by COSMO-RS calculations.

IL-coated supported Ir(CO) ₂ complexes	Solubility of each component in IL at 333 K (capacity, mol/mol)					
	BD	T2B	1B	C2B	B	H ₂
[BMIM][NTf ₂]	0.90	0.46	0.50	0.49	0.23	1.95
[BMIM][BF ₄]	0.24	0.13	0.15	0.14	0.06	1.20
[DMIM][MSO ₄]	0.80	0.38	0.41	0.39	0.20	1.65
[BMIM][TFA]	0.50	0.24	0.26	0.25	0.12	1.46
[EMIM][DEP]	0.68	0.37	0.39	0.38	0.21	1.75
[DMIM][DMP]	1.04	0.57	0.61	0.59	0.33	1.95
[BMIM][Ac]	0.72	0.44	0.47	0.45	0.27	1.75

References

- (1) Babucci, M.; Uzun, A., *J. Molec. Liq.* **2016**, 216, 293-297.
- (2) Ravel, B.; Newville, M., *J. Synchrotron Rad.* **2005**, 12, 537-541.
- (3) Newville, M., *J. Synchrotron Rad.* **2001**, 8, 322-324.
- (4) Lu, J.; Serna, P.; Gates, B. C., *ACS Catal.* **2011**, 1, 1549-1561.
- (5) Jalal, A.; Uzun, A., *J. Catal.* **2017**, 350, 86-96.
- (6) Anantharaj, R.; Banerjee, T., *Ind. Eng. Chem. Res.* **2010**, 49, 8705-8725.
- (7) Lu, J.; Aydin, C.; Browning, N. D.; Gates, B. C., *Langmuir* **2012**, 28, 12806-12815.
- (8) Martinez-Macias, C.; Chen, M.; Dixon, D. A.; Gates, B. C., *Chem. Eur. J.* **2015**, 21, 11825-11835.
- (9) Ravi, A.; Sheppard, N., *J. Phys. Chem.* **1972**, 76, 2699-2703.